

# Recalibrating the Wide-field Infrared Survey Explorer (WISE) W4 Filter

M. J. I. Brown<sup>1,2,3</sup>, T. H. Jarrett<sup>4</sup>, and M. E. Cluver<sup>5</sup>

<sup>1</sup>School of Physics, Monash University, Clayton, Victoria 3800, Australia

<sup>2</sup>Monash Centre for Astrophysics, Monash University, Clayton, Victoria, 3800, Australia

<sup>3</sup>ARC Future Fellow

<sup>4</sup>Department of Astronomy, University of Cape Town, Private Bag X3, Rondebosch 7701, South Africa

<sup>5</sup>University of the Western Cape, Robert Sobukwe Road, Bellville, 7535, South Africa

## Abstract

We present a revised effective wavelength and photometric calibration for the Wide-field Infrared Survey Explorer (WISE) *W4* band, including tests of empirically motivated modifications to its pre-launch laboratory-measured relative system response curve. We derived these by comparing measured *W4* photometry with photometry synthesised from spectra of galaxies and planetary nebulae. The difference between measured and synthesised photometry using the pre-launch laboratory-measured *W4* relative system response can be as large as 0.3 mag for galaxies and 1 mag for planetary nebulae. We find the *W4* effective wavelength should be revised upward by 3.3%, from 22.1  $\mu\text{m}$  to 22.8  $\mu\text{m}$ , and the *W4* AB magnitude of Vega should be revised from  $m_{W4} = 6.59$  to  $m_{W4} = 6.66$ . In an attempt to reproduce the observed *W4* photometry, we tested three modifications to the pre-launch laboratory-measured *W4* relative system response curve, all of which have an effective wavelength of 22.8  $\mu\text{m}$ . Of the three relative system response curve models tested, a model that matches the laboratory-measured relative system response curve, but has the wavelengths increased by 3.3% (or  $\simeq 0.73 \mu\text{m}$ ) achieves reasonable agreement between the measured and synthesised photometry.

**Keywords:** infrared: general – infrared: galaxies – galaxies: photometry – (ISM:) planetary nebulae: general – space vehicles: instruments

## 1 Introduction

The Wide-field Infrared Survey Explorer (WISE; Wright et al. 2010) surveyed the entire sky in four passbands, which were intended to have effective wavelengths of 3.4, 4.6, 12 and 22  $\mu\text{m}$ . The two reddest filters, *W3* and *W4*, are useful for constraining the thermal emission from objects with temperatures of several hundred Kelvin (e.g., Mainzer et al. 2011a,b; Wu et al. 2012). The *W4* filter also provides a star formation rate indicator for nearby galaxies that should be comparable in accuracy to *Spitzer* 24  $\mu\text{m}$  (e.g., Kennicutt et al. 2009; Jarrett et al. 2013; Cluver et al. 2014).

Unfortunately, the pre-launch laboratory-measured WISE *W4* relative system response (RSR) curve does not match its on-sky performance (Wright et al. 2010). As WISE photometry was calibrated using A stars and K-M giants (Jarrett et al. 2011), by construction objects with spectral indices between 1 and 2 (where the spectral index is defined by  $f_\nu \propto \nu^\alpha$ ) have accurate photometry. However, the AB magnitudes and flux densi-

ties for star-forming galaxies and active galactic nuclei with spectral indices of  $\alpha < 0$  are systematically in error.

Wright et al. (2010) found that the fluxes of star-forming galaxies (with spectra approximated by  $f_\nu \propto \nu^{-2}$ ) were overestimated by 9%. Brown et al. (2014) found the error is a smooth function of 22  $\mu\text{m}$  spectral index, with the error approaching 30% for some ultra-luminous infrared galaxies (ULIRGS). Wright et al. (2010) concluded that the flux errors could be resolved by shifting the effective wavelength of the *W4* filter redward by 2% to 3%.

The aim of this paper is to define an accurate effective wavelength, photometric calibration, and practical RSR model for the WISE *W4* filter. For filters with effective wavelengths of  $\sim 22 \mu\text{m}$ , the AB magnitudes of Vega were determined using a single-temperature Kurucz model for Vega (Kurucz 1991; Cohen et al. 1992), incorporating a 2.7% increase in the fluxes as described by Cohen (2009). This Vega basis has an overall systematic uncertainty of  $\simeq 1.45\%$  (Cohen et al. 1992).

The resulting AB magnitude of Vega is  $m_{22} = 5.81$  in the *Spitzer* IRS Peak-Up Imager red channel and  $m_{24} = 6.67$  in the *Spitzer* MIPS 24  $\mu\text{m}$  band. In general we use Vega-based magnitudes, with all exceptions being explicitly noted in the text.

## 2 Effective Wavelength

In this paper we define apparent magnitudes using

$$m = -2.5 \log \left[ \left( \int R(\nu) \frac{f_\nu(\nu)}{h\nu} d\nu \right) \times \left( \int R(\nu) \frac{g_\nu(\nu)}{h\nu} d\nu \right)^{-1} \right] \quad (1)$$

(e.g., Hogg et al. 2002) where  $f_\nu$  is the SED of the source,  $g_\nu$  is the SED of a  $m = 0$  source (either Vega or  $f_\nu = 3631$  Jy),  $R_\nu$  is the filter response function (defined as electrons per incident photon) and  $h\nu$  is the energy of a photon with frequency  $\nu$ . Please note that these magnitudes are based on photon counts rather than fluxes, and do not simply correspond to monochromatic flux densities at the effective wavelengths of the relevant filters.

Brown et al. (2014) quantified the systematic error in the WISE *W4* photometry by comparing measured photometry with synthetic photometry derived from galaxy spectral energy distributions. The Brown et al. (2014) sample spans a broad range of galaxy types, including early-type galaxies, late-type galaxies, luminous infrared galaxies, starbursts, Seyferts and blue compact dwarfs. The top-left panel of Figure 1 shows the anomaly as a function of  $\sim 22 \mu\text{m}$  spectral index,  $\alpha_{22}$ .

The residual is well approximated by

$$\Delta m_{W4} = (0.035 \pm 0.001) \times (\alpha_{22} - 2) \quad (2)$$

with an RMS of 0.05 magnitudes (Brown et al. 2014). This residual is much larger than the flux corrections discussed by Wright et al. (2010), which were intended for derivations of monochromatic flux densities from *W4* photometry. For a minority of objects with measured  $\alpha_{22}$  or with an assumed  $\alpha_{22}$ , Equation 2 can be used to correct WISE *W4* photometry so that it matches the pre-launch RSR curve (e.g., Brown et al. 2014). For the majority of objects that lack known  $\alpha_{22}$  values, we need a revised effective wavelength and WISE *W4* RSR model.

We can use Equation 2 to derive the revised effective wavelength for the *W4* filter. If the pre-launch effective wavelength and actual effective wavelengths correspond to frequencies of  $\nu_0$  and  $\nu_1$  respectively, then

$$\Delta m_{W4} \simeq -2.5 \log \left( \frac{f_\nu(\nu_1)}{g_\nu(\nu_1)} \right) + 2.5 \log \left( \frac{f_\nu(\nu_0)}{g_\nu(\nu_0)} \right) \quad (3)$$

$$\Delta m_{W4} \simeq 2.5 \log \left( \frac{f_\nu(\nu_0) g_\nu(\nu_1)}{g_\nu(\nu_0) f_\nu(\nu_1)} \right) \quad (4)$$

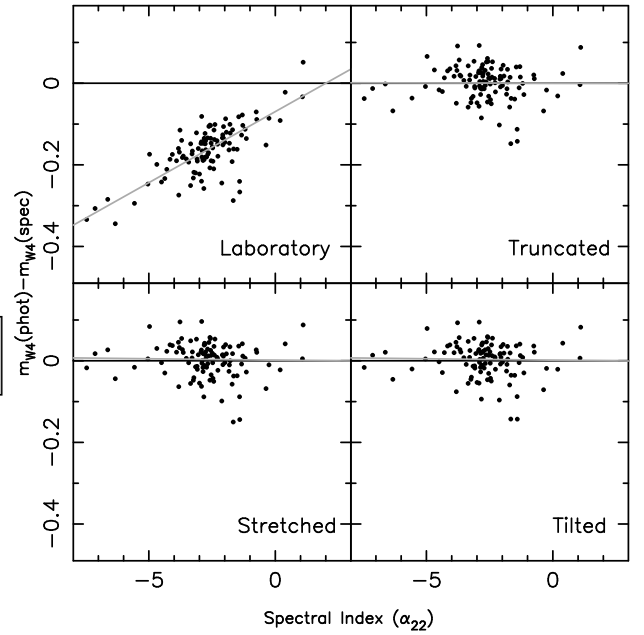


**Figure 1.** The difference between measured and synthesised *W4* magnitudes for galaxies drawn from Brown et al. (2014), plotted as a function of  $\sim 22 \mu\text{m}$  spectral index. The top-left panel shows that the pre-launch laboratory-measured WISE *W4* RSR does not match the on-sky performance (Wright et al. 2010; Jarrett et al. 2011), so the measured *W4* magnitudes are systematically too bright for galaxies with spectra that differ significantly from the Rayleigh-Jeans approximation. All three modified filter curves reduce the discrepancy between the measured and synthesised *W4* magnitudes, with the stretched and tilted filter response curves performing best.

If  $g_\nu$  is a Rayleigh-Jeans spectrum and  $f_\nu$  is a power-law with index  $\alpha_{22}$  then

$$\Delta m_{W4} \simeq 2.5 \log \left( \frac{f_\nu(\nu_0) g_\nu(\nu_0) \nu_1^2 \nu_0^{-2}}{g_\nu(\nu_0) f_\nu(\nu_0) \nu_1^\alpha \nu_0^{-\alpha}} \right) \quad (5)$$

$$(0.035 \pm 0.001) \times (\alpha_{22} - 2) \simeq 2.5 \log \left( \frac{\nu_0^{(\alpha_{22}-2)}}{\nu_1^{(\alpha_{22}-2)}} \right) \quad (6)$$

$$(0.035 \pm 0.001) \simeq 2.5 \log \left( \frac{\nu_0}{\nu_1} \right) \quad (7)$$

Equation 7 shows the *W4* effective wavelength should be revised upward by  $3.3 \pm 0.1\%$ , from  $22.1 \mu\text{m}$  (Wright et al. 2010) to  $22.8 \mu\text{m}$ . The *W4* filter can be considered, to first order, a  $23 \mu\text{m}$  passband. The corresponding AB magnitude of Vega in the *W4* band is revised from  $m_{W4} = 6.59$  to  $m_{W4} = 6.66$ . When updating existing WISE catalogues to use the new effective wavelength, Vega-based magnitudes can remain unchanged in value, but AB magnitudes (and SED dependent monochromatic flux densities) must account for the revised AB magnitude of Vega.

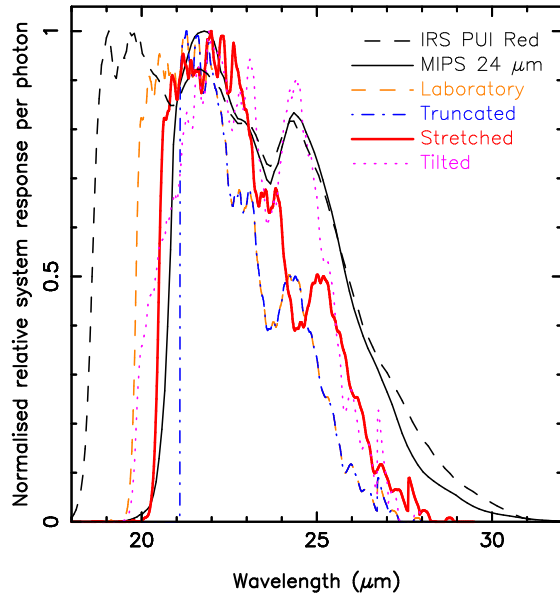


**Figure 2.** The laboratory-measured  $W4$  RSR, the three modified  $W4$  RSRs, the *Spitzer* IRS Peak-Up Imager red channel ( $22.3 \mu\text{m}$ ) RSR and the MIPS  $24 \mu\text{m}$  RSR. All of the RSRs are renormalised so the RSRs peak at 1.00.

### 3 RSR Models and Galaxies

To compare observed and model spectral energy distributions with observed  $W4$  photometry, a revised  $W4$  RSR model is needed. We have tested the pre-launch laboratory-measured  $W4$  RSR and three alternative  $W4$  RSR models to determine which provides the best agreement between measured photometry and photometry synthesised from spectra. All three alternative  $W4$  RSR models have an effective wavelength of  $22.8 \mu\text{m}$ .

The truncated RSR model is identical to the laboratory-measured RSR except it has zero transmission below a wavelength of  $21.1 \mu\text{m}$ . The stretched RSR is identical to the laboratory-measured RSR except all the wavelengths have been revised upward by 3.3% (i.e.,  $\Delta\lambda = 0.033\lambda$ ). Please note that comparisons of measured and synthesised photometry using the stretched RSR and a modified laboratory-measured RSR with the wavelengths increased by  $0.73 \mu\text{m}$  (i.e.,  $\Delta\lambda = 0.73 \mu\text{m}$ ) were equivalent within our uncertainties. The tilted RSR is the product of the laboratory-measured RSR multiplied by a function that increases linearly from 0 to 1 between  $18.6 \mu\text{m}$  and  $28 \mu\text{m}$  wavelength. All of the RSRs used in this paper are plotted in Figure 2.

We used the Brown et al. (2014) *Spitzer* IRS-LL spectra and models of galaxies to generate synthetic pho-

tometry for the laboratory-measured  $W4$  RSR and the three alternative  $W4$  RSR models, and then compared this to the measured matched aperture photometry of Brown et al. (2014). As we illustrate in Figure 1, all three modified  $W4$  RSRs produce excellent agreement between measured photometry and photometry synthesised from spectra for galaxies, with no significant residual as a function spectral index.

### 4 RSR Models and Planetary Nebulae

To further discriminate between the RSR models, we have measured the mid-infrared colours of bright planetary nebulae with WISE  $W4$  and *Spitzer* MIPS  $24 \mu\text{m}$  filters, and compared these with colours synthesised from *Spitzer* IRS-LL spectroscopy. While galaxy spectra are dominated by a (relatively) featureless continuum near  $23 \mu\text{m}$ , planetary nebulae often feature a prominent [OIV] emission line at  $25.9 \mu\text{m}$ . Although the planetary nebulae spectra in the  $W4$  wavelength range are dominated by a single emission line, the magnitudes still depend on the shape of the entire  $W4$  RSR as they are normalised with a model Vega spectrum. As the [OIV] emission line is far from the effective wavelength of the  $W4$  filter, it is non-trivial to convert AB magnitudes (defined by Equation 1) into monochromatic flux densities.

Planetary nebulae from the NGC and IC catalogues were selected from Kohoutek (2001), and these were then cross matched with data in the *Spitzer Heritage Archive*<sup>1</sup> and the Cornell Atlas of *Spitzer*/IRS Sources (CASSIS; Lebouteiller et al. 2011). *Spitzer* IRS-LL spectra of planetary nebulae are typically “stare mode” spectra rather than “spectral maps”, so we could not easily match our photometric aperture with the spectroscopic extraction aperture. However, the stare mode spectra were sufficient to check that the planetary nebulae selected had weak continua and strong [OIV] emission. We also attempted to use supernova remnants, but found most of the objects with IRS-LL spectra had relatively strong continua and weak [OIV] emission, so we excluded them from our analysis.

The final sample of planetary nebulae was NGC 246, NGC 3587, NGC 6720, NGC 6852, NGC 6853 and NGC 7293, and the renormalised spectra are plotted in Figure 3. The photometry of the planetary nebulae was measured using large rectangular apertures as in Brown et al. (2014), and this photometry is provided in Table 1. We have not removed stellar contamination from the planetary nebula photometry, but stars only significant alter the photometry well short-ward of the  $W4$  filter. As all of the planetary nebulae are very bright, we expect systematic errors (e.g., calibration errors) to dominate over photon Poisson noise.

<sup>1</sup><http://sha.ipac.caltech.edu/>

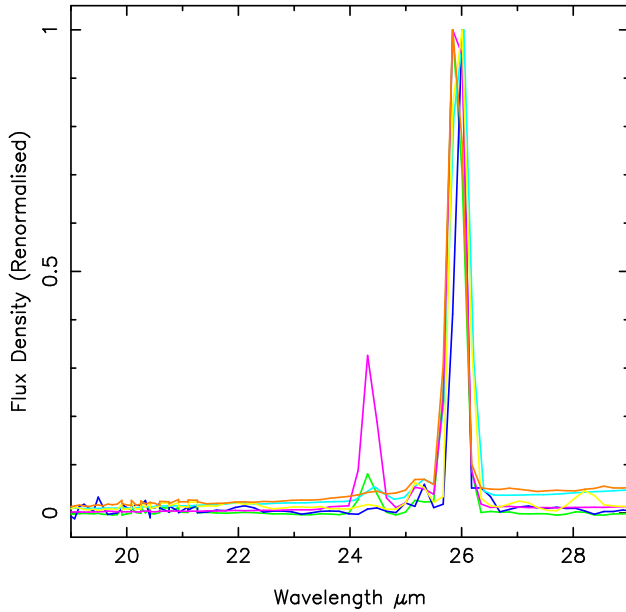


**Figure 3.** The *Spitzer* IRS-LL planetary nebula spectra used for testing the shape of the *W4* RSR. To aid the comparison of the spectra, they have all been renormalised using the peak of the [OIV] emission line at  $25.9 \mu\text{m}$ . All of the planetary nebulae have weak continuum emission and strong [OIV] emission, and some of the nebulae feature the [NeV] emission line at  $24.3 \mu\text{m}$ .

In Figure 4 we compare the measured  $m_{W4} - m_{24}$  colours of planetary nebula with colours synthesised from spectra. There are gross offsets between the measured colours and those synthesised from the laboratory RSR and the truncated RSR. Smaller offsets are seen between measured colours and those synthesised from the tilted RSR, while there is good agreement between the measured and synthesised photometry for stretched RSR. Both the tilted and stretched RSRs effectively increase transmission at the red end of the filter (i.e., they are consistent with a “red leak”).

The *Spitzer* IRS Peak-Up Imager red channel ( $22.3 \mu\text{m}$ ) allows us to cross check the measured and synthesised colours of planetary nebulae without relying on calibration of the MIPS  $24 \mu\text{m}$  band, although we can undertake this test for just one object in our sample. The measured colour of NGC 6852 is  $m_{22} - m_{W4} = 0.86$ , while a single  $25.9 \mu\text{m}$  emission line produces  $m_{22} - m_{W4}$  colours of  $-0.22$ ,  $0.28$ ,  $0.93$  and  $0.65$  for the laboratory-measured, truncated, stretched and tilted RSRs (respectively). This is consistent with our tests using  $m_{W4} - m_{24}$  colours, where the best agreement between measured and synthesised colours was for the stretched RSR.

We caution that only three RSR models are presented in this paper, and our stretched RSR is unlikely to be a unique solution for resolving the discrepancy between measured and synthesised *W4* photometry. We also cau-

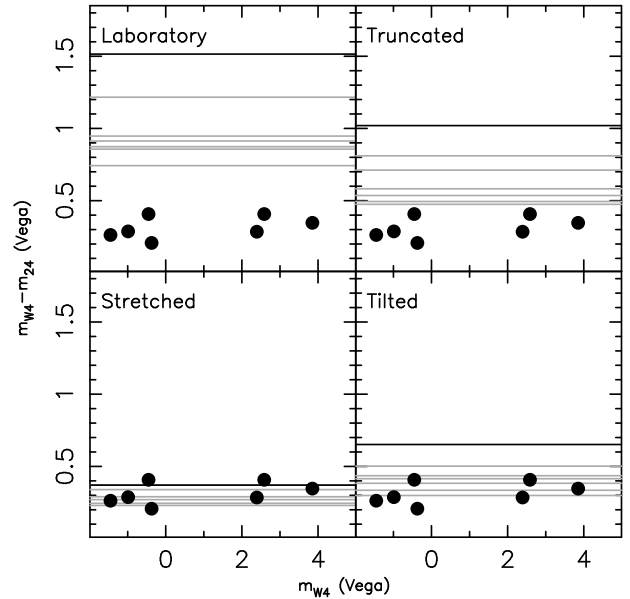


**Figure 4.** The measured  $m_{W4} - m_{24}$  colours of planetary nebula and colours synthesised from spectra. The black solid line denotes a spectrum with a single  $25.9 \mu\text{m}$  emission line while the grey lines are synthesised from *Spitzer* IRS-LL spectra of planetary nebulae. Of the RSRs tested, the stretched filter response curve provides the best agreement between the measured photometry and photometry synthesised from spectra.

tion that while the stretched RSR provides the best agreement between the measured and synthesised *W4* photometry, an error in transmission or quantum efficiency is far more likely than a wavelength error. The stretched filter curve should thus be considered a useful empirical model for comparing *W4* photometry with spectra, rather than a unique physical description of the *W4* RSR.

## 5 Summary

We present a revised effective wavelength, photometric calibration, and RSR models for the WISE *W4* filter, derived using comparisons of measured photometry and photometry synthesised from galaxy and planetary nebula spectra. The on-sky performance of the WISE *W4* RSR does not match pre-launch laboratory measurements, resulting in large flux density errors for star-forming galaxies, active galactic nuclei and planetary nebulae.

The offset between the measured *W4* photometry and photometry synthesised from spectra is a function of  $22 \mu\text{m}$  spectral index. When spectral index information is available, Equation 2, can be used to adjust measured photometry so it is on the system defined by the pre-launch laboratory-measured RSR.

When spectral index information is not available, a revised effective wavelength must be used (although

Vega-based magnitudes remain unchanged). We find the effective wavelength of the W4 filter should be revised upward by 3.3%, from 22.1  $\mu\text{m}$  to 22.8  $\mu\text{m}$ . The corresponding AB magnitude of Vega in the W4 band should be revised from  $m_{W4} = 6.59$  to  $m_{W4} = 6.66$ . The W4 filter can be considered, to first order, a 23  $\mu\text{m}$  pass-band.

To compare spectral energy distributions with observed W4 photometry, a revised W4 RSR model is needed. Using galaxy spectra, we could not easily distinguish between different models of the W4 RSR that all have an effective wavelength of 22.8  $\mu\text{m}$ . The prominent 25.9  $\mu\text{m}$  [OIV] emission line in planetary nebula spectra allowed us to distinguish between three possible W4 RSR models. Of the three RSR models tested, we find that a RSR that matches the shape laboratory-measured curve, but with the wavelengths increased by 3.3% (or increased by  $\simeq 0.73$   $\mu\text{m}$ ) adequately reconciles measured photometry and photometry synthesised from spectra.

## 6 ACKNOWLEDGEMENTS

MB acknowledges financial support from the Australian Research Council (FT100100280) and the Monash Research Accelerator Program (MRA). TJ and MC would like to acknowledge the support of the South African National Research Foundation and Department of Science and Technology. This publication makes use of data products from the Wide-field Infrared Survey Explorer, which is a joint project of the University of California, Los Angeles, and the Jet Propulsion Laboratory/California Institute of Technology, funded by the National Aeronautics and Space Administration. This work is based in part on observations made with the *Spitzer* Space Telescope, obtained from the NASA/IPAC Infrared Science Archive, both of which are operated by the Jet Propulsion Laboratory, California Institute of Technology under a contract with the National Aeronautics and Space Administration. The Cornell Atlas of *Spitzer*/IRS Sources (CASSIS) is a product of the Infrared Science Center at Cornell University, supported by NASA and JPL.

## REFERENCES

Brown, M. J. I., Moustakas, J., Smith, J.-D. T., da Cunha, E., Jarrett, T. H., Imanishi, M., Armus, L., Brandl, B. R., & Peek, J. E. G. 2014, *ApJS*, 212, 18  
 Cluver, M. E., Jarrett, T. H., Hopkins, A. M., Driver, S. P., Liske, J., Gunawardhana, M. L. P., Taylor, E. N., Robotham, A. S. G., Alpaslan, M., Baldry, I., Brown, M. J. I., Peacock, J. A., Popescu, C. C., Tuffs, R. J., Bauer, A. E., Bland-Hawthorn, J., Colless, M., Holwerda, B. W., Lara-Lopez, M. A., Leschinski, K., Lopez-Sanchez, A. R., Norberg, P., Owers, M., Wang, L., & Wilkins, S. M. 2014, *ArXiv e-prints*  
 Cohen, M. 2009, *AJ*, 137, 3449

Cohen, M., Walker, R. G., Barlow, M. J., & Deacon, J. R. 1992, *AJ*, 104, 1650  
 Hogg, D. W., Baldry, I. K., Blanton, M. R., & Eisenstein, D. J. 2002, *ArXiv Astrophysics e-prints*  
 Jarrett, T. H., Cohen, M., Masci, F., Wright, E., Stern, D., Benford, D., Blain, A., Carey, S., Cutri, R. M., Eisenhardt, P., Lonsdale, C., Mainzer, A., Marsh, K., Padgett, D., Petty, S., Ressler, M., Skrutskie, M., Stanford, S., Surace, J., Tsai, C. W., Wheelock, S., & Yan, D. L. 2011, *ApJ*, 735, 112  
 Jarrett, T. H., Masci, F., Tsai, C. W., Petty, S., Cluver, M. E., Assef, R. J., Benford, D., Blain, A., Bridge, C., Donoso, E., Eisenhardt, P., Koribalski, B., Lake, S., Neill, J. D., Seibert, M., Sheth, K., Stanford, S., & Wright, E. 2013, *AJ*, 145, 6  
 Kennicutt, Jr., R. C., Hao, C.-N., Calzetti, D., Moustakas, J., Dale, D. A., Bendo, G., Engelbracht, C. W., Johnson, B. D., & Lee, J. C. 2009, *ApJ*, 703, 1672  
 Kohoutek, L. 2001, *A&A*, 378, 843  
 Kurucz, R. L. 1991, in *Precision Photometry: Astrophysics of the Galaxy*, ed. A. G. D. Philip, A. R. Uggren, & K. A. Janes, 27  
 Leboutteiller, V., Barry, D. J., Spoon, H. W. W., Bernard-Salas, J., Sloan, G. C., Houck, J. R., & Weedman, D. W. 2011, *ApJS*, 196, 8  
 Mainzer, A., Grav, T., Masiero, J., Bauer, J., Wright, E., Cutri, R. M., McMillan, R. S., Cohen, M., Ressler, M., & Eisenhardt, P. 2011a, *ApJ*, 736, 100  
 Mainzer, A., Grav, T., Masiero, J., Bauer, J., Wright, E., Cutri, R. M., Walker, R., & McMillan, R. S. 2011b, *ApJ*, 737, L9  
 Wright, E. L., Eisenhardt, P. R. M., Mainzer, A. K., Ressler, M. E., Cutri, R. M., Jarrett, T., Kirkpatrick, J. D., Padgett, D., McMillan, R. S., Skrutskie, M., Stanford, S. A., Cohen, M., Walker, R. G., Mather, J. C., Leisawitz, D., Gautier, III, T. N., McLean, I., Benford, D., Lonsdale, C. J., Blain, A., Mendez, B., Irace, W. R., Duval, V., Liu, F., Royer, D., Heinrichsen, I., Howard, J., Shannon, M., Kendall, M., Walsh, A. L., Larsen, M., Cardon, J. G., Schick, S., Schwalm, M., Abid, M., Fabinsky, B., Naes, L., & Tsai, C.-W. 2010, *AJ*, 140, 1868  
 Wu, J., Tsai, C.-W., Sayers, J., Benford, D., Bridge, C., Blain, A., Eisenhardt, P. R. M., Stern, D., Petty, S., Assef, R., Bussmann, S., Comerford, J. M., Cutri, R., Evans, II, N. J., Griffith, R., Jarrett, T., Lake, S., Lonsdale, C., Rho, J., Stanford, S. A., Weiner, B., Wright, E. L., & Yan, L. 2012, *ApJ*, 756, 96

Table 1 Planetary nebula photometry

Name	J2000 Coordinates	Photometric Aperture	$m_{W1}^a$	$m_{W2}$	$m_{W3}$	$m_{22}$	$m_{W4}$	$m_{24}$
NGC 246	00:47:04 -11:52:14.1	$300'' \times 300''$	7.99	7.84	3.68	-	-0.96	-1.28
NGC 3587	11:14:47 +55:01:06.6	$100'' \times 100''$	10.68	10.37	5.83	-	3.88	3.51
NGC 6720	18:53:34 +33:01:48.2	$120'' \times 120''$	7.84	7.14	2.62	-	-0.34	-0.58
NGC 6852	20:00:39 +01:43:43.5	$45'' \times 45''$	14.23	10.65	6.40	3.45	2.59	2.18
NGC 6853	19:59:37 +22:43:26.4	$480'' \times 480''$	5.00	4.43	1.40	-	-1.42	-1.71
NGC 7293	22:29:39 -20:50:09.7	$1200'' \times 1200''$	5.13	4.55	0.95	-	-0.42	-0.86

<sup>a</sup>Foreground and background stars were not subtracted from the images, and can contribute significantly to the  $W1$  and  $W2$  photometry.